## Title

# *Myoparr*-associated and -independent multiple roles of heterogeneous nuclear ribonucleoprotein K during skeletal muscle cell differentiation

## Authors

Keisuke Hitachi[1], Yuri Kiyofuji[1], Masashi Nakatani[2], and Kunihiro Tsuchida[1,*]

## Affiliations

[1]Division for Therapies against Intractable Diseases, Institute for Comprehensive Medical Science (ICMS), Fujita Health University, Toyoake, Japan, [2]Faculty of Rehabilitation and Care, Seijoh University, Tokai, Japan

*Correspondence: tsuchida@fujita-hu.ac.jp

## Abstract

RNA-binding proteins (RBPs) regulate cell physiology via the formation of ribonucleic-protein complexes with coding and non-coding RNAs. RBPs have multiple functions in the same cells; however, the precise mechanism through which their pleiotropic functions are determined remains unknown. In this study, we revealed the multiple inhibitory functions of heterogeneous nuclear ribonucleoprotein K (hnRNPK) for myogenic differentiation. We first identified hnRNPK as a lncRNA *Myoparr* binding protein. Gain- and loss-of-function experiments showed that hnRNPK repressed the expression of *myogenin* at the transcriptional level. The hnRNPK-binding region of

*Myoparr* was required to repress *myogenin* expression. Moreover, hnRNPK repressed the expression of a set of genes coding for aminoacyl-tRNA synthetases in a *Myoparr*-independent manner. Mechanistically, hnRNPK regulated the eIF2α/Atf4 pathway, one branch of the intrinsic pathways of the endoplasmic reticulum sensors, in differentiating myoblasts. Thus, our findings demonstrate that hnRNPK plays lncRNA-associated and -independent multiple roles during myogenic differentiation, indicating that the analysis of lncRNA-binding proteins will be useful for elucidating both the physiological functions of lncRNAs and the multiple functions of RBPs.

**Keywords**

transcriptional regulation, myogenic differentiation, RNA-binding protein, endoplasmic reticulum stress

## Introduction

Long non-coding RNAs (lncRNAs), which are >200 nucleotides (nt) in length and which do not encode more than 100 amino acids, are emerging as important regulators in diverse biological processes, including transcription, splicing, RNA stability, and translation (Statello et al., 2021). LncRNAs are pervasively transcribed from the noncoding genomic DNA; cis-regulatory regions, including promoter and enhancer, introns, 3' untranslated regions, and repetitive sequences (Chakraborty et al., 2014). LncRNAs are also expressed from the antisense direction of the coding genomic DNA (Hon et al., 2017). Thus, most of the genomic regions have the potential to express lncRNAs. Thus far, more than 260,000 lncRNA genes are registered in the LncBook, which is a curated knowledge-based database for human lncRNAs (Ma et al., 2019). Since lncRNAs exert their molecular functions by interacting with proteins, mRNAs, or microRNAs (Hitachi and Tsuchida, 2020), their molecular functions differ widely, depending on the interacting partners.

As lncRNA-interacting factors, RNA-binding proteins (RBPs) are essential to determine the molecular function of each lncRNA (Statello et al., 2021). In the human genome, more than 1,500 genes encode RBPs (Gerstberger et al., 2014). RBPs consist of ribonucleoprotein complexes together with lncRNAs to regulate various biological aspects. For example, the association of Ddx5/Ddx17 with lncRNAs, such as *SRA*, *mrhl*, *MeXis*, or *Myoparr*, is required to activate the expression of downstream genes (Caretti et al., 2006; Hitachi et al., 2019; Kataruka et al., 2017; Sallam et al., 2018). RBPs, including NONO, SFPQ, FUS, and RBM14, associate with *Neat1*, which is a highly abundant lncRNA in mammals, to form a large membrane-less structure paraspeckle in the nucleus (Hirose et al., 2019). A ubiquitously expressed RBP, known as human antigen

R (HuR) associates with lncRNAs and regulates their stability; HuR increases the cytosolic *linc-MD1* levels in skeletal muscle cells (Legnini et al., 2014), whereas it promotes the decay of *lincRNA-p21* in HeLa cells (Yoon et al., 2012). Additionally, RBPs are also involved in RNA splicing, polyadenylation, RNA transport, and translation (Kelaini et al., 2021). The majority of RBPs are involved in multiple biological processes in concert with lncRNAs (Briata and Gherzi, 2020; Jonas et al., 2020; Nostrand et al., 2020), and mutations in genes coding for RBPs are associated with human genetic disorders (Gebauer et al., 2021).

Heterogeneous nuclear ribonucleoprotein K (hnRNPK), a member of the heterogeneous nuclear ribonucleoprotein family, has multiple roles, including chromatin remodeling, transcription, RNA splicing, and translation (Bomsztyk et al., 2004; Wang et al., 2020). hnRNPK acts together with *lincRNA-p21*, *EWSAT1*, and *lncRNA-OG*, to regulate the expression of downstream genes in mouse embryonic fibroblasts, Ewing sarcoma, and bone marrow-derived mesenchymal stem cells (Dimitrova et al., 2014; Howarth et al., 2014; Tang et al., 2018). However, the molecular function of hnRNPK in skeletal muscle cells has not been fully elucidated. LncRNA *Myoparr* is an essential regulator of skeletal muscle cell proliferation and differentiation (Hitachi et al., 2019). *Myoparr* shares the same promoter region with the *myogenin* gene and activates *myogenin* expression by promoting the interaction between Ddx17 and histone acetyltransferase PCAF (Hitachi et al., 2019). We previously identified hnRNPK as a candidate for *Myoparr*-associated protein in skeletal muscle cells (Hitachi et al., 2019), suggesting the unique functions of *Myoparr*-associated hnRNPK during myogenic differentiation. In the present study, we revealed the inhibitory role of hnRNPK as a *Myoparr*-associated protein in skeletal muscle cell differentiation. Moreover, by comparing the downstream genes

regulated by *Myoparr* and hnRNPK, we also found a *Myoparr*-independent role of hnRNPK during myogenic differentiation. Our findings reveal that hnRNPK plays *Myoparr*-associated and -independent multiple roles in skeletal muscle cell differentiation and will contribute to elucidating the complex roles of RBPs in cell differentiation.

## Materials and Methods

### Cell cultures, siRNA transfection, and ISRIB treatment

A mouse myoblast cell line, C2C12, was cultured in Dulbecco's modified Eagle medium (DMEM) supplemented with 10% fetal bovine serum at 37°C under 5% $CO_2$. Myogenic differentiation was induced by replacing the medium with the differentiation medium, DMEM supplemented with 2% horse serum. C2C12 myoblasts were transfected with 50 nM of Stealth RNAi (Thermo Fisher Scientific, Waltham, MA, USA) using Lipofectamine 3000 (Thermo Fisher Scientific) according to the manufacturer's protocol. The following siRNAs were used: Stealth RNAi siRNA negative control (Negative Control, Med GC, Thermo Fisher Scientific), stealth RNAi for *Myoparr*, and stealth RNAi siRNAs specific for *hnRNPK* (MSS205172 and MSS205173, Thermo Fisher Scientific). The siRNA sequences are listed in Supplemental Table 1. At 24 h after siRNA transfection, myogenic differentiation was induced. At 24 h or 72 h after differentiation induction, cells were collected for the analysis of RNAs and proteins. For ISRIB treatment, the differentiation medium was added either with or without 1 μM ISRIB (Cayman Chemical Company, Ann Arbor, MI, USA).

### RNA isolation, reverse transcription reaction, and quantitative RT-PCR

Total RNA was extracted from C2C12 cells using ISOGEN II reagent (Nippon Gene, Tokyo, Japan) according to the manufacturer's protocol. After DNase I (Thermo Fisher Scientific) treatment, total RNA was used for reverse transcription reaction using SuperScript III Reverse Transcriptase (Thermo Fisher Scientific) or ProtoScript II Reverse Transcriptase (New England Biolabs (NEB), Beverly, MA, USA) with random or oligo (dT) primers (Thermo Fisher Scientific). Quantitative real-time PCR was conducted using SYBR Premix Ex Taq (Takara Bio Inc., Shiga, Japan) and a Thermal Cycler Dice Real Time System TP800 (Takara Bio Inc.). The results were normalized to the *Rpl26* expression. The primers used are listed in Supplementary Table 1.

**Protein extraction and Western blotting**

Cells were lysed in RIPA buffer (50 mM Tris-HCl (pH 8.0), 150 mM NaCl, 0.1% SDS, 1% Triton X-100, 0.5% sodium deoxycholate) containing protease inhibitors (1 mM phenylmethylsulfonyl fluoride, 1 μg/ml aprotinin, 4 μg/ml leupeptin) and phosphatase inhibitors (5 mM NaF, 5 mM β-glycerophosphate, 1 mM $Na_3VO_4$). The protein concentration was measured using a Pierce BCA Protein Assay Kit (Thermo Fischer Scientific). Equal amounts of protein were used for Western blotting. The following primary antibodies were used: myogenin antibody (F5D) (sc-12732, Santa Cruz Biotechnology, Dallas, TX, USA), MHC antibody (MF20, Developmental Studies Hybridoma Bank (DSHB)), Myod antibody (CE-011A, Cosmo Bio Co. Ltd., Tokyo, Japan), hnRNPK antibody (#4675, Cell Signaling Technology (CST), Beverly, MA, USA), hnRNPK antibody (F45P9C7, BioLegend, San Diego, CA, USA), TIAR antibody (#8509, CST), and Atf4 antibody (693901, BioLegend). The following HRP-linked secondary antibodies were used: anti-mouse IgG (#7076, CST), anti-rabbit IgG (#7074,

CST), and TrueBlot ULTRA anti-Ig HRP, Mouse (Rat) (18-8817-33, Rockland Immunochemicals Inc., Limerick, PA, USA). Can Get Signal Immunoreaction Enhancer Solution (Toyobo, Osaka, Japan) was used when necessary. The signal was detected with ImmunoStar LD reagent (FUJIFILM Wako, Osaka, Japan) using a cooled CCD camera system (Light-Capture, ATTO, Tokyo, Japan).

**Immunofluorescence assay**

Immunofluorescence analyses of C2C12 cells were performed as previously described (Hitachi et al., 2019). Briefly, 24 h or 72 h after the induction of differentiation, cells were fixed with 4% PFA and permeabilized with 0.2% Triton X-100. After blocking with 5% FBS, cells were stained with an anti-myogenin antibody (F5D, DSHB) or with an anti-MHC antibody (MF20, DSHB). The following secondary antibodies were used: Goat anti-Mouse IgG (H+L) Highly Cross-Adsorbed Secondary Antibody, Alexa Fluor 488 (Thermo Fisher Scientific). Nuclei were counterstained with DAPI (Dojindo, Kumamoto, Japan). A DMI4000B microscope with a DFC350FX CCD camera (Leica, Wetzlar, Germany) was used for visualization of signals. Images were analyzed using the Image J software program (ver. 1.53a).

**Identification of *Myoparr*-binding proteins**

*Myoparr*-binding proteins were collected with the RiboTrap Kit (Medical & Biological Laboratories (MBL), Aichi, Japan) using BrU labeled RNAs, as described previously (Hitachi et al., 2019). BrU-labeled *Myoparr* and *EGFP* RNA were prepared using the Riboprobe System (Promega, Madison, WI, USA). Twenty-four hours after the induction of differentiation, nuclear extract was prepared from differentiating C2C12

158 myoblasts. The *Myoparr* or *EGFP* RNA (50 pmol) were mixed with the nuclear extract
159 from differentiating C2C12 myoblasts for 2 h at 4°C. The RNA-protein complexes were
160 collected by Protein G Plus Agarose (Thermo Fisher Scientific) conjugated to an anti-
161 BrdU antibody, and proteins were eluted by adding BrdU. Purified proteins were detected
162 by Western blotting using a specific antibody, as described above.
163
164 **RNA immunoprecipitation and the RNA pull-down assay**
165 Immunoprecipitation of endogenous RNAs (*Myoparr*, *Xist*, or *Neat1*) was
166 performed using the RIP-Assay Kit (MBL) using $2 \times 10^7$ C2C12 cells 48 h after the
167 induction of differentiation, as previously described (Hitachi et al., 2019). The following
168 antibodies were used for RNA immunoprecipitation: normal rabbit IgG (#2729S, CST),
169 anti-HNRNPK pAb (RN019P, MBL), or TIAR mAb (#8509, CST). After treatment with
170 DNase I, immunoprecipitated RNAs was used for the reverse transcription reaction. The
171 precipitation percentage (precipitated RNA vs. input RNA) was calculated by qRT-PCR
172 using the primers listed in Supplementary Table 1.
173 An RNA pull-down assay was performed with a RiboTrap Kit. Various lengths
174 of *Myoparr* were subcloned into a pGEM-Teasy vector (Promega). BrU-labeled *Myoparr*
175 (10 pmol each) was bound to Protein G Plus Agarose conjugated to an anti-BrdU antibody
176 and mixed with the *in vitro* transcribed/translated hnRNPK protein. After several washing
177 steps, the binding of hnRNPK to *Myoparr* was analyzed by Western blotting using an
178 hnRNPK antibody as described above.
179
180 **Luciferase reporter assay**
181 The upstream region of *myogenin* (-1650/+51) was PCR-amplified and cloned

182 into the pGL4.20 vector (Promega). The *hnRNPK*-expressing plasmid was a kind gift
183 from Dr. H. Okano (Yano et al., 2005). Proliferating C2C12 cells were transfected with
184 the *myogenin* promoter and *hnRNPK*-expressing plasmid using Lipofectamine 2000
185 (Thermo Fisher Scientific). The total amount of DNA was kept constant by the addition
186 of the pcDNA3 vector. Cells were collected at 24 h after the induction of differentiation
187 and dissolved in Passive Lysis Buffer (Promega). The effect of hnRNPK on *myogenin*
188 promoter was measured using a Lumat LB 9507 luminometer (Berthold Technologies,
189 Bad Wildbad, Germany) with the Dual-Luciferase Reporter Assay System (Promega)
190 according to the manufacturer's protocol. The pGL4.74 vector (Promega) was used as an
191 internal control. The relative luciferase activity is shown as the firefly to Renilla luciferase
192 ratio.

193 To reconstitute the complex chromatin structure and epigenetic regulation *in*
194 *vitro* (Liu et al., 2001), the upstream regions of *myogenin* (-242/+51 and -1650/+51) were
195 subcloned into the episomal luciferase vector, pREP4-luc, and the -242-Luc and -1650-
196 Luc constructs were generated. To create the -1650Δccawmcc-Luc construct, the
197 upstream region (-971/-902) of *myogenin* was deleted from the -1650-Luc construct. The
198 region containing the putative hnRNPK-binding motif ccawmcc was identified by
199 RBPmap (Paz et al., 2014). The episomal luciferase vector, pREB7-Rluc, was used as an
200 internal control for the luciferase assay. The pREP4-luc and pREP7-Rluc vectors were
201 gifts from Dr. K. Zhao (Liu et al., 2001). Subconfluent C2C12 cells were transfected with
202 the indicated episomal luciferase vectors using Lipofectamine 2000. After myogenic
203 induction, cells were collected and used to measure the relative luciferase activity.
204

205 **Analysis of downstream genes regulated by *Myoparr* KD and *hnRNPK* KD**

206 Downstream genes regulated by *Myoparr* KD and *hnRNPK* KD were identified as
207 described previously (Hitachi and Tsuchida, 2019) using our RNA-Seq raw data
208 (accession No. DRA005527). Briefly, statistical analysis of differentially expressed genes
209 by *Myoparr* KD and *hnRNPK* KD was performed using DESeq2 ver. 1.12.4 software
210 (Love et al., 2014) with a Wald test (cut-offs: false discovery rate (adjusted *p*-value, padj)
211 < 0.05 and log 2 fold change > 0.75 or < -0.75). A pathway analysis of significantly
212 upregulated genes coding for cytosolic aminoacyl-tRNA synthetases was performed
213 based on the KEGG (Kanehisa et al., 2020). A Gene Ontology (GO) analysis of
214 differentially expressed genes was performed with DAVID ver. 6.8
215 (https://david.ncifcrf.gov/). An enrichment analysis was performed using Metascape
216 (Zhou et al., 2019).
217
218 **Statistical analysis**
219 Error bars represent standard deviation. Statistical analyses were performed
220 using unpaired two-tailed Student's *t*-tests. For comparisons of more than 2 groups, a one-
221 way ANOVA followed by Tukey's post hoc test was performed using Prism 9 (GraphPad
222 Software, San Diego, CA, USA). Statistical significance is reported in the Figures and
223 Figure legends. *P* values of < 0.05 were considered statistically significant.
224
225 **Results**
226 **Identification of hnRNPK as a *Myoparr*-binding protein in skeletal muscle cells**
227 Our proteomics analysis identified both hnRNPK and TIAR as candidates for
228 *Myoparr*-associated proteins (Hitachi et al., 2019). To reveal whether hnRNPK and TIAR
229 are associated with the *Myoparr* function during myogenic differentiation, we first

examined the specific interaction of *Myoparr* with endogenous hnRNPK and TIAR. *In vitro* synthesized *Myoparr* was labeled with 5-bromouridine (BrU) and mixed with the nuclear extract from differentiating C2C12 myoblasts. After purification of *Myoparr* by immunoprecipitation with a BrdU antibody, specific binding between *Myoparr* and hnRNPK protein was confirmed by immunoblotting (Figure 1A). Since binding between *EGFP* mRNA and hnRNPK was not observed, *EGFP* mRNA was used as a negative control. Intracellular binding between endogenous *Myoparr* and hnRNPK was shown by RNA immunoprecipitation using an hnRNPK-specific antibody without a crosslinking (Figure 1B and C). This enrichment of *Myoparr* by hnRNPK was stronger than that of *Xist* or *Neat1*, both of which interact with hnRNPK in other cells (Chu et al., 2015; Kawaguchi et al., 2015). Although TIAR protein was retrieved by synthesized *Myoparr*, intracellular endogenous interaction between *Myoparr* and TIAR was not observed (Supplementary Figure 1A-C). These results suggested that hnRNPK has function associated with *Myoparr*-binding during skeletal muscle differentiation.

**hnRNPK represses the expression of *myogenin* in differentiating myoblasts**

During myogenic differentiation, the expression of *Myoparr* gradually increases and is required to activate the expression of *myogenin* (Hitachi et al., 2019). Thus, we examined the changes in the expression of hnRNPK during C2C12 cell differentiation. Although the expression of myogenin was highly increased after myogenic induction, the expression of hnRNPK gradually decreased (Figure 2A), suggesting the regulatory role of hnRNPK in the expression of *myogenin*. We next knocked down *hnRNPK* using the small interfering RNAs (siRNAs) in differentiating C2C12 cells. An immunocytochemistry analysis of the myogenin expression after

*hnRNPK* knockdown (KD) by two distinct siRNAs did not show a sufficient increase in the ratio of myogenin-positive cells comparing to the control (Figure 2B). However, we observed that the number of cells with high intensity of myogenin signal was increased by *hnRNPK* KD (Figure 2B and C). In addition, western blotting analyses showed that *hnRNPK* KD was associated with a significant increase in the expression of myogenin (Figure 2D-F). These results indicated that although *hnRNPK* KD is not enough to induce the expression of myogenin in cells where the expression of myogenin is not intrinsically present, *hnRNPK* KD increases the expression of myogenin in cells with intrinsic myogenin expression.

We observed that the expression of *myogenin* was significantly increased by *hnRNPK* KD (Figure 2G and H). Although the differences were not statistically significant, the *Myoparr* expression levels also tended to be increased by *hnRNPK* KD (Figure 2I). From these results, we surmise that hnRNPK negatively regulates the expression of *myogenin* at the transcriptional level. The effect of hnRNPK on the transcription of *myogenin* was examined using the *myogenin*-promoter-driven luciferase assay. The overexpression of hnRNPK in differentiating C2C12 cells decreased the *myogenin* promoter activity (Figure 2J), indicating that hnRNPK negatively regulates the expression of *myogenin* via the *myogenin* promoter.

**The hnRNPK-binding region of *Myoparr* is required to repress *myogenin* expression**

The hnRNPK-binding region of *Myoparr* was determined by RNA pull-down experiments using the various forms of *Myoparr* (Figure 3A). Figure 3B showed that hnRNPK bound to the full-length sense-strand of *Myoparr* (#3 in Figure 3B), but not to the full-length antisense-strand of *Myoparr* (#4). Although deletion of the 5'-region (#5

and 6) or 3'-region (#2 and 7) of *Myoparr* did not affect binding to hnRNPK, the deletion of the 3'-half of *Myoparr* (#1) completely diminished the binding to hnRNPK (Figure 3B). These results indicated that an approximately 300-nt region (613-952 nt) of *Myoparr* is indispensable for binding to hnRNPK. Searching the motif sequence of RBPs from the 300-nt region revealed that there are 8 ccawmcc motifs, which are recognized by hnRNPK (Figure 3C). The deletion of the motifs (660-729 nt) from the full-length of *Myoparr* (#8) markedly weakened the binding to hnRNPK (Figure 3B). Thus, the ccawmcc motifs on *Myoparr* were shown to be required for binding to hnRNPK.

To clarify whether *Myoparr* is involved in regulating the expression of *myogenin* by hnRNPK, we examined the effect of the ccawmcc motif on the *myogenin* promoter activity. To imitate a chromatin structure and epigenetic regulation on the plasmid DNA (Liu et al., 2001), the upstream region of *myogenin* (-1649 to +52) including *Myoparr* was cloned into an episomal luciferase vector. In accordance with our previous findings (Hitachi et al., 2019), the *myogenin* promoter showed high activity in the presence of *Myoparr* (-1650-Luc) in comparison to the -242-Luc construct, which only contains the *myogenin* promoter region in differentiating myoblasts (Figure 3D). Intriguingly, the activity of the -1650-Luc construct was further enhanced by the deletion of a region of approximately 70 bp (1650Δccawmcc-Luc), which corresponds to the 660-729 nt region on *Myoparr* (Figure 3D). These results indicate that the hnRNPK-binding region of *Myoparr* is required to repress the expression of *myogenin* during skeletal muscle differentiation.

**hnRNPK inhibits skeletal muscle differentiation but is required for normal myotube formation**

The inhibitory role of hnRNPK in the expression of *myogenin* possibly via the ccawmcc motif on *Myoparr* suggested that hnRNPK and *Myoparr* have common downstream genes. Our RNA-Seq analysis (Hitachi and Tsuchida, 2019) revealed that *hnRNPK* KD significantly increased the expression of 226 genes and significantly decreased the expression of 190 genes. We compared the downstream genes regulated by *hnRNPK* KD and *Myoparr* KD, and the comparative heatmap analysis showed that the genes regulated by *hnRNPK* KD showed the opposite direction to the *Myoparr* KD (Figure 4A). Twenty percent of genes (84/416) altered by *hnRNPK* KD overlapped with genes regulated by the *Myoparr* KD (Figure 4B and Supplementary Talbe 2). The intersection of these genes was 12.3-fold greater than that expected by chance ($p = 1.393037 \times 10^{-45}$). Although these 84 genes showed a low correlation coefficient (R=0.0758323), we observed a negative correlation trend for one segment of them, including *myogenin*; the expression of 50 genes belonging to this segment was increased by *hnRNPK* KD and decreased by *Myoparr* KD (red frame in Figure 4C). These genes were enriched in sarcomere organization, myofibril assembly, and muscle contraction categories in GO terms (Figure 4D), indicating that hnRNPK inhibits myogenic differentiation and maturation.

In accordance with the results of the RNA-Seq analysis, we observed a significant increase in the expression of Myod, one of master regulators of myogenesis, and Myosin heavy chain (MHC), which is a later marker of myogenic differentiation and maturation, in the early stages of differentiation with *hnRNPK* KD (Figure 4E), indicating the *hnRNPK* KD causes premature differentiation of myoblasts. Although *hnRNPK* KD increased MHC expression in the late stages of differentiation (Figure 4F), *hnRNPK* KD did not affect the percentage of differentiated cells; this was shown by the fusion index

(Figure 4G) as well as the results from immunocytochemistry to detect myogenin (Figure 2C). Instead, we observed the appearance of locally spherical myotubes following *hnRNPK* KD. These differed from the normal tube-shaped myotubes (Figure 4G). Thus, these results indicated that hnRNPK is required for normal myotube formation, possibly through the inhibitory effect on the premature differentiation of myoblasts at early stages of differentiation.

**hnRNPK represses the expression of aminoacyl-tRNA synthetases via the eIF2α/Atf4 pathway**

The Venn diagram in Figure 4B indicates that 332 genes regulated by *hnRNPK* KD were *Myoparr*-independent, suggesting the *Myoparr*-independent role of hnRNPK in differentiating myoblasts. We performed an enrichment analysis of genes regulated by *hnRNPK* KD and compared them with genes regulated by *Myoparr* KD. As reported previously (Hitachi et al., 2019), genes related to cell cycle and cell division were only enriched in genes regulated by *Myoparr* KD (Figure 5A). Skeletal muscle-associated genes were regulated by both *Myoparr* KD and *hnRNPK* KD (Figure 5A). Intriguingly, genes coding for aminoacyl-tRNA synthetases were regulated specifically by *hnRNPK* KD (red frame in Figure 5A). In mice, there are two-types of aminoacyl-tRNA synthetases: cytosolic and mitochondrial aminoacyl-tRNA synthetase. Our RNA-Seq analysis showed that *hnRNPK* KD significantly increased the expression of 10 genes coding for cytosolic aminoacyl-tRNA synthetases, whereas it had little effect on the expression of genes coding for mitochondrial aminoacyl-tRNA synthetases (Supplementary Figure 2). To confirm the RNA-Seq results, we randomly picked up 5 genes coding for cytosolic aminoacyl-tRNA synthetases, and their expression changes by

350 *hnRNPK* KD were verified by qRT-PCR. *hnRNPK* KD using two distinct siRNAs
351 significantly increased the expression of *Aars*, *Gars*, *Iars*, *Nars*, and *Sars* (Figure 5B-F).
352 This regulation was not observed following *Myoparr* KD (Figure 5B-F), indicating that
353 hnRNPK regulates the expression of these genes in a *Myoparr*-independent manner.

354 The expression of genes coding for almost all cytosolic aminoacyl-tRNA
355 synthetases is activated by transcription factor Atf4 (Harding et al., 2003; Shan et al.,
356 2016). Thus, we examined whether *hnRNPK* KD altered the expression of Atf4 in skeletal
357 muscle cells. Although not statistically significant, the *Atf4* expression in differentiating
358 myoblasts tended to be increased by *hnRNPK* KD (Figure 5G). *Myoparr* KD did not affect
359 the expression of *Atf4* (Figure 5G). The effect of *hnRNPK* KD was more pronounced in
360 the expression of Atf4 protein. The amount of Atf4 protein was highly increased by
361 *hnRNPK* KD (Figure 5H). We further examined the expression changes of other ATF4
362 target genes by *hnRNPK* KD in differentiating myoblasts. The expression levels of *Asns*
363 and *Psat1*, which encode proteins related to amino acid synthesis, were significantly
364 increased by *hnRNPK* KD (Supplementary Figure 3A and B). In addition, the expression
365 levels of *Chop*, *Chac1*, and *Trb3*, pro-apoptosis genes, and *Gadd34*, an another ATF4
366 target gene, also tended to be increased by *hnRNPK* KD (Supplementary Figure 3C-F).
367 These results suggest that hnRNPK regulates the expression of genes associated with
368 amino acid synthesis via the expression of Atf4.

369 Under the condition of endoplasmic reticulum (ER) stress, *Atf4* mRNA is
370 translated more efficiently and contributes to the restoration of cell homeostasis via the
371 regulation of cytosolic aminoacyl-tRNA synthetases (Afroze and Kumar, 2017). Thus, to
372 reveal the molecular mechanism by which hnRNPK regulates the expression of Atf4, we
373 finally focused on ER stress. ISRIB is an inhibitor of eIF2α, which is a downstream

374 component of PERK signaling, one branch of the ER stress sensors. We investigated
375 whether ISRIB treatment could suppress the increase in the expression of Atf4 induced
376 by *hnRNPK* KD and found that ISRIB treatment completely rescued this *hnRNPK*-KD-
377 induced increase (Figure 6A). Furthermore, ISRIB treatment abrogated the increased
378 expression of Atf4 target genes, *Aars*, *Gars*, *Iars*, *Nars*, and *Sars* by *hnRNPK* KD (Figure
379 6B-F and Supplementary Figure 4A-E). Thus, these results indicate that *Myoparr*-
380 independent hnRNPK function is the regulation of the eIF2α/Atf4 pathway during
381 myogenic differentiation.
382
383 **Discussion**
384 RBPs have multiple molecular functions, including RNA splicing, transcription,
385 translation, RNA stability, and the formation of the nuclear structure, to regulate cell
386 proliferation, differentiation, development, and diseases (Kelaini et al., 2021). Although
387 many RBPs have multiple functions in the cells (Briata and Gherzi, 2020; Jonas et al.,
388 2020; Nostrand et al., 2020), it is still unclear how their pleiotropic functions are
389 determined. In this study, we revealed novel multiple functions of hnRNPK, a member of
390 the hnRNP family of RBPs, in skeletal muscle cells. By focusing on a lncRNA *Myoparr*-
391 associated protein, we found that hnRNPK repressed the expression of *myogenin*, coding
392 for one of the master regulators of muscle differentiation. Deletion of the hnRNPK-
393 binding region of *Myoparr* activated the expression of *myogenin*. Moreover, our
394 comparative analysis of the downstream genes of hnRNPK and *Myoparr* showed that the
395 function of hnRNPK was pleiotropic. During myogenic differentiation, hnRNPK
396 repressed the expression of a set of genes coding for cytosolic aminoacyl-tRNA
397 synthetases via the eIF2α/Atf4 pathway. Taken together, our study revealed multiple

398 inhibitory roles of hnRNPK in skeletal muscle cells: one was *Myoparr*-associated and the
399 other was *Myoparr*-independent (Figure 7). Recently, Xu et al. reported that the
400 deficiency of 36 amino acids in hnRNPK diminished C2C12 differentiation (Xu et al.,
401 2018). However, our results provided strong evidence to support that hnRNPK has an
402 inhibitory effect on muscle differentiation. In addition, we observed the appearance of
403 locally spherical myotubes following *hnRNPK* KD. Considering the facts that
404 dysregulated Myod expression leads to premature myogenic differentiation (Bröhl et al.,
405 2012) and results in the formation of dysfunctional myofibers in mice (Schuster-Gossler
406 et al., 2007), uncoordinated increases in Myod, myogenin, and MHC expression by
407 *hnRNPK* KD may lead to abnormal shape of myotubes. In addition, the morphology of
408 these myotubes closely resembles myotubes with myofibril-assembly defects (Wang et
409 al., 2013), suggesting that hnRNPK may also be involved in the regulation of the
410 myofibril assembly in myotubes. Therefore, despite its lncRNA-associated and -
411 independent roles in the inhibition of myogenic differentiation, hnRNPK is apparently
412 required for the formation of normal myotubes.

413 We observed that *hnRNPK* KD increased myogenin protein levels more
414 robustly than *myogenin* mRNA. The peak expression of myogenin protein is detected 1-
415 2 days after that of *myogenin* mRNA in both *in vitro* and *in vivo* myogenesis (Angelis et
416 al., 1992; Figueroa et al., 2003), suggesting that a slight increase in *myogenin* mRNA by
417 *hnRNPK* KD in the early stages of myogenic differentiation eventually led to a marked
418 increase in myogenin protein. Therefore, the fine-tuning of the *myogenin* expression by
419 hnRNPK at the early stages of differentiation may have a significant impact on the overall
420 myogenic differentiation processes through the RNA-protein network. Intriguingly,
421 despite the percentage of myogenin-positive cells was not changed, the expression of

myogenin protein was increased by *hnRNPK* KD. We observed that *hnRNPK* KD only increased the number of cells with high intensity of myogenin signal. These results suggest that hnRNPK can specifically repress the expression of *myogenin* in a subset of responding cells, rather than by simply turning off the expression of *myogenin* in every myoblast. Our experiments showed that hnRNPK repressed the expression of *myogenin* at the transcriptional level possibly via binding to the ccawmcc motif on *Myoparr*, suggesting that the existence of *Myoparr* would be necessary for hnRNPK to inhibit the expression of *myogenin*. Since *myogenin* and *Myoparr* share the same promoter region (Hitachi et al., 2019), *myogenin* and *Myoparr* are likely expressed in the same cells. Thus, the expression of *myogenin* would not be activated in the cells without the cell-intrinsic expression of *Myoparr*, even if *hnRNPK* is depleted in every myoblast. Further studies are required to investigate the more precise molecular mechanism by which hnRNPK regulates the expression of *myogenin* via binding to *Myoparr*.

ER stress is induced by several perturbations disrupting cell homeostasis, including protein misfolding, viral infection, and changes in intracellular calcium concentration (Hetz et al., 2015). The cells recognize those stresses with three branches of ER transmembrane sensors signaling, PERK, inositol-requiring protein 1 (IRE1), and ATF6 (Afroze and Kumar, 2017). During myogenic differentiation, ATF6 signaling was activated and led to apoptosis in myoblasts (Nakanishi et al., 2005). The increased phosphorylation of eIF2α, a component of PERK signaling, was observed in myoblasts at the early stage after the induction of differentiation (Alter and Bengal, 2011). In addition, treatment with ER stress inducers enhanced apoptosis in myoblasts but led to efficient myogenic differentiation in the remaining surviving cells (Nakanishi et al., 2007). Recently, the deletion of PERK in satellite cells, which are adult muscle stem cells, was

446 shown to inhibit myogenic differentiation and led to impaired skeletal muscle
447 regeneration in adult mice (Xiong et al., 2017), indicating that ER stress promotes
448 myogenic differentiation. In this study, we showed that the *hnRNPK* KD in differentiating
449 myoblasts increased the expression of Atf4 and this effect was diminished by treatment
450 with ISRIB, a specific inhibitor of eIF2α. The expression levels of a set of genes coding
451 for cytosolic aminoacyl-tRNA synthetases, which are regulated by Atf4, were also
452 increased by the *hnRNPK* KD, and were completely rescued after ISRIB treatment. The
453 inhibitory effects of hnRNPK on Atf4 and cytosolic aminoacyl-tRNA synthetases were
454 independent of *Myoparr*. Therefore, our findings suggest that hnRNPK fine-tunes the
455 myogenic differentiation process by modulating ER stress via eIF2α/Atf4 signaling in a
456 lncRNA-independent manner. Since hnRNPK is involved in the translational efficiency
457 (Lynch et al., 2005; Yano et al., 2005), a decrease in hnRNPK may induce the unfolded
458 protein response via the translational machinery in myoblasts and alter eIF2α/Atf4
459 signaling.

460 In conclusion, hnRNPK plays multiple lncRNA-dependent and -independent
461 roles in the inhibition of myogenic differentiation. Thus, the analysis of RBPs bound to
462 lncRNAs will be useful for elucidating both the physiological functions of lncRNAs and
463 the complex functions of RBPs in cell differentiation. Induced ER stress, including
464 increased PERK signaling, was observed in skeletal muscle biopsy samples from
465 myotonic dystrophy 1 patients and in mdx mice, a model of Duchenne muscular
466 dystrophy (Hulmi et al., 2016; Ikezoe et al., 2007). Moreover, mutations in genes coding
467 for aminoacyl-tRNA synthetases are implicated in human neuromuscular disorders
468 (Benarroch et al., 2020), and autoantibodies against aminoacyl-tRNA synthetases are
469 found in autoimmune disease (Targoff et al., 1993). Collectively, downstream genes of

hnRNPK are strongly associated with neuromuscular and other disorders in humans, suggesting that targeting hnRNPK to regulate the expression of these genes and signaling may become a new therapeutic strategy for human diseases.

**Acknowledgments**

This work was supported in part by JSPS KAKENHI (19H03427 and 20K07315), Intramural Research Grants (2-5) for Neurological and Psychiatric Disorders of NCNP, and a Grant-in-Aid from the Mochida Memorial Foundation for Medical and Pharmaceutical Research.

**Author Contributions**

K.H. and K.T. designed research; K.H. analyzed data; K.H., Y.K., and M.N. performed research; K.H. and K.T. wrote the paper. All authors revised, edited, and read the manuscript and approved the final manuscript.

**Conflict of interest**

The authors declare no competing interests in association with the present study.

**Figure Legends**

**Figure 1. Intracellular interaction between *Myoparr* and hnRNPK in differentiating C2C12 cells.** (A) Synthesized *Myoparr* was mixed with C2C12 nuclear extract. Following purification of *Myoparr* by immunoprecipitation, the interaction between *Myoparr* and hnRNPK was confirmed by immunoblotting using an hnRNPK-specific antibody. *EGFP* mRNA was used for the control. Note that the smaller band would be a

494 splicing isoform of hnRNPK (Makeyev and Liebhaber, 2002). (B) RNA
495 immunoprecipitation for *Myoparr*, *Xist*, and *Neat1* in differentiating C2C12 cells by an
496 hnRNPK antibody. The interaction between endogenous *Myoparr* and hnRNPK was
497 detected by qRT-PCR 2 days after the differentiation induction. Normal rabbit IgG was
498 used for the control. The presence or absence of reverse transcription reaction is shown
499 by (RT+) or (RT-), respectively. n = 4, mean ± SD. ***$p < 0.001$. (C) hnRNPK protein
500 from C2C12 cells purified by immunoprecipitation in (B) was confirmed by Western
501 blotting.
502
503 **Figure 2. hnRNPK represses the expression of myogenin at the transcriptional level.**
504 (A) Western blots showing the hnRNPK and myogenin expression during C2C12
505 differentiation. The tubulin expression served as an internal control. (B)
506 Immunocytochemistry for myogenin 48 h after *hnRNPK* KD in C2C12 cells. Nuclei were
507 counterstained with DAPI. Bar, 100 μm. The percentage of the myogenin-positive cells
508 is shown as the percentage of the control. n = 4, mean ± SD. n.s., not significant. (C) The
509 results of the cell count based on the signal intensity of immunocytochemistry for
510 myogenin of (B). The red line indicates the median. Control; n=824, *hnRNPK* siRNA-1;
511 n=859, *hnRNPK* siRNA-2; n=761. ***$p < 0.001$. A Mann–Whitney nonparametric test
512 was used for comparisons between each group. (D) Western blots showing increased
513 myogenin expression in C2C12 cells 48 h after *hnRNPK* KD. Blots are representative of
514 four repeats. (E-F) Relative quantification of hnRNPK (E) and myogenin (F) from (D). n
515 = 4, mean ± SD. ***$p < 0.001$, **$p < 0.01$. (G-I) Quantitative RT-PCR to detect the
516 expression of *hnRNPK* (G), *myogenin* (H), and *Myoparr* (I) after *hnRNPK* knockdown. n
517 = 3-4, mean ± SD. ***$p < 0.001$, *$p < 0.05$, n.s., not significant. (J) Exogenous hnRNPK

518 decreased the promoter activity of *myogenin* in differentiating C2C12 cells. n = 3, mean
519 ± SD. **p* < 0.05.
520
521 **Figure 3. The hnRNPK region on *Myoparr* is required for repression of *myogenin***
522 **promoter activity.** (A) A schematic diagram of various lengths of *Myoparr* used for RNA
523 pull-down assays. (B) *In vitro* transcribed/translated hnRNPK protein was pulled down
524 by *Myoparr* and then detected by Western blotting using an hnRNPK-specific antibody.
525 Lane numbers are consistent with (A). The RNA lanes indicate various forms of *Myoparr*
526 used for RNA pull-down. (C) The results of an RBPmap analysis searching the motif of
527 hnRNPK. Colored letters correspond to the hnRNPK motif. The red frame indicates the
528 ccawmcc motifs within the region deleted in Δccawmcc, #8 in (A). (D) The left panel
529 shows a schematic diagram of the constructs used for the luciferase assays. -242-Luc
530 contains the *myogenin* promoter region. -1650-Luc contains both the *myogenin* promoter
531 region and *Myoparr*. -1650Δccawmcc-Luc contains the *myogenin* promoter region and
532 *Myoparr* without the ccawmcc motifs, corresponding to #8 in A. The right panel shows
533 the relative luciferase activities of indicated constructs in differentiating C2C12 cells. n
534 = 4, mean ± SD. ****p* < 0.001, ***p* < 0.01, **p* < 0.05.
535
536 **Figure 4. hnRNPK inhibits myogenic differentiation but is required for normal**
537 **myotube formation.** (A) A heatmap diagram showing the increased or decreased
538 expression of genes regulated by *Myoparr* KD and *hnRNPK* KD. (B) The intersection of
539 genes regulated by *Myoparr* KD and *hnRNPK* KD shows a significant (Fisher's exact test)
540 overlap, which is 12.3 times larger than would be expected by chance alone. (C) Eighty-
541 four genes with expression levels that were significantly altered by both *Myoparr* KD and

542 *hnRNPK* KD showed an un-correlated pattern (R = 0.0758323, log 2 ratio scale). The red
543 frame indicates the 50 genes for which the expression was decreased by *Myoparr* KD but
544 increased by *hnRNPK* KD. (D) Enrichment GO categories of the 50 genes, corresponding
545 to the red frame in (C). (E) Western blots showing increased MHC and Myod expression
546 in C2C12 cells 48 h after *hnRNPK* KD. Blots are representative of three repeats. (F)
547 Western blot showing the increased expression of MHC in C2C12 myotubes 96 h after
548 *hnRNPK* KD. The tubulin expression served as an internal control. The blots shown are
549 representative of three experiments. (G) Immunocytochemistry for MHC 96 h after
550 *hnRNPK* KD. Nuclei were counterstained with DAPI. Bar, 100 μm. The fusion index is
551 shown as the percent of the control. n = 3, mean ± SD. n.s., not significant.
552
553 **Figure 5. hnRNPK regulates the expression of genes coding for aminoacyl-tRNA**
554 **synthetases in a *Myoparr*-independent manner.** (A) A Metascape analysis of genes
555 regulated by *Myoparr* KD and *hnRNPK* KD. The red frame indicates the GO terms that
556 were specifically enriched in *hnRNPK* KD. (B-G) qRT-PCR to detect the expression of
557 *Aars* (B), *Gars* (C), *Iars* (D), *Nars* (E), *Sars* (F), *Atf4* (G) after either *Myoparr* KD or
558 *hnRNPK* KD. n = 3, mean ± SD. $^{**}p < 0.01$, $^{*}p < 0.05$, n.s., not significant. (H) Western
559 blot showing the increased expression of Atf4 by *hnRNPK* KD. The tubulin expression
560 served as an internal control. Blots are representative of three experiments.
561
562 **Figure 6. hnRNPK regulates the expression of genes coding for aminoacyl-tRNA**
563 **synthetases via the eIF2α/Atf4 pathway.** (A) Western blot showing the increased Atf4
564 expression after *hnRNPK* KD, and ISRIB treatment suppressed the increase. DMSO is
565 used as a control. The blots shown are representative of three experiments. (B-F) qRT-

PCR to detect the expression of *Aars* (B), *Gars* (C), *Iars* (D), *Nars* (E), *Sars* (F) after *hnRNPK* KD and ISRIB treatment. n = 3, mean ± SD. $^{**}p < 0.01$, $^{*}p < 0.05$, n.s., not significant.

**Figure 7. Multiple inhibitory roles of hnRNPK during myogenic differentiation.** During myogenic differentiation, hnRNPK has two different downstream targets. One is *myogenin*, which codes for a regulator of myogenic differentiation. hnRNPK represses the *myogenin* expression by binding to the ccawmcc motifs on *Myoparr*. The other target is aminoacyl-tRNA synthetases. hnRNPK regulates the expression of aminoacyl-tRNA synthetases via the eIF2α/Atf4 pathway. In hnRNPK-depleted cells, the hyperactivated expression of these genes may lead to the locally spherical formation of myotubes.

**Supplementary Table 1.** Primer and siRNA sequences.

**Supplementary Table 2.** The value (log2 fold change) of the genes for which expression levels were increased or decreased by *Myoparr* KD and *hnRNPK* KD.

**Supplementary Figure 1. Detection of the interaction between *Myoparr* and TIAR in differentiating C2C12 cells.** (A) The interaction between synthesized *Myoparr* and TIAR was detected by immunoblotting using a TIAR antibody. (B) qRT-PCR for the detection of *Myoparr* and *Xist* following RNA-immunoprecipitation using a TIAR antibody. The presence or absence of reverse transcription reaction is shown by (RT+) or (RT-), respectively. Bars indicate the average of two independent experiments, and circles and triangles represent the values of each experiment. (C) Purified TIAR protein from

C2C12 cells by immunoprecipitation using a TIAR antibody was confirmed by Western blotting.

**Supplementary Figure 2. RNA-Seq revealed the altered expression of a group of genes coding for cytosolic aminoacyl-tRNA synthetases by *hnRNPK* KD.** (A) The KEGG pathway diagram of cytosolic aminoacyl-tRNA biosynthesis. The gene names surrounded by the red frame indicate genes that are significantly upregulated by *hnRNPK* KD. (B-C) The results of the RNA-Seq analysis showing the altered expression of genes coding for cytosolic aminoacyl-tRNA synthetases (B) and mitochondrial aminoacyl-tRNA synthetases (C) by *hnRNPK* KD. Red and blue indicate genes that are significantly upregulated or downregulated, respectively, by *hnRNPK* KD.

**Supplementary Figure 3. The expression changes of ATF4 target genes by *hnRNPK* KD in differentiating myoblasts.** (A-F) The results of qRT-PCR for detecting the expression of *Asns* (A), *Psat1* (B), *Gadd34* (C), *Chop* (D), *Chac1* (E), and *Trb3* (F) following *hnRNPK* KD. n = 3, mean ± SD. $^{***}p < 0.001$, $^{*}p < 0.05$.

**Supplementary Figure 4. hnRNPK regulates the expression of a group of genes coding for aminoacyl-tRNA synthetases via the eIF2α/Atf4 pathway.** (A-E) The results of qRT-PCR for detecting the altered expression of *Aars* (A), *Gars* (B), *Iars* (C), *Nars* (D), and *Sars* (E) following *hnRNPK* KD (using a different siRNA from Figure 6) and ISRIB treatment. n = 3, mean ± SD. $^{*}p < 0.05$.

**References**

614 **Afroze, D. and Kumar, A.** (2017). ER stress in skeletal muscle remodeling and
615 myopathies. *Febs J* **286**, 379-398.
616 **Alter, J. and Bengal, E.** (2011). Stress-induced C/EBP Homology Protein (CHOP)
617 represses MyoD transcription to delay myoblast differentiation. *Plos One* **6**, e29498.
618 **Angelis, M. G. C.-D., Lyons, G., Sonnino, C., Angelis, L. D., Vivarelli, E., Farmer, K.,**
619 **Wright, W. E., Molinaro, M., Bouchè, M. and Buckingham, M.** (1992). MyoD,
620 myogenin independent differentiation of primordial myoblasts in mouse somites. *J*
621 *Cell Biology* **116**, 1243-1255.
622 **Benarroch, L., Bonne, G., Rivier, F. and Hamroun, D.** (2020). The 2021 version of the
623 gene table of neuromuscular disorders (nuclear genome). *Neuromuscular Disord* **30**,
624 1008-1048.
625 **Bomsztyk, K., Denisenko, O. and Ostrowski, J.** (2004). hnRNP K: One protein multiple
626 processes. *Bioessays* **26**, 629-638.
627 **Briata, P. and Gherzi, R.** (2020). Long non-coding RNA-ribonucleoprotein networks in
628 the post-transcriptional control of gene expression. *Non-coding Rna* **6**, 40.
629 **Bröhl, D., Vasyutina, E., Czajkowski, M. T., Griger, J., Rassek, C., Rahn, H.-P.,**
630 **Purfürst, B., Wende, H. and Birchmeier, C.** (2012). Colonization of the satellite
631 cell niche by skeletal muscle progenitor cells depends on Notch signals. *Dev Cell* **23**,
632 469-481.
633 **Caretti, G., Schiltz, R. L., Dilworth, F. J., Padova, M. D., Zhao, P., Ogryzko, V.,**
634 **Fuller-Pace, F. V., Hoffman, E. P., Tapscott, S. J. and Sartorelli, V.** (2006). The
635 RNA helicases p68/p72 and the noncoding RNA SRA are coregulators of MyoD and
636 skeletal muscle differentiation. *Dev Cell* **11**, 547-560.
637 **Chakraborty, S., Deb, A., Maji, R. K., Saha, S. and Ghosh, Z.** (2014). LncRBase: An
638 enriched resource for lncRNA information. *Plos One* **9**, e108010.
639 **Chu, C., Zhang, Q. C., da Rocha, S. T., Flynn, R. A., Bharadwaj, M., Calabrese, J.**
640 **M., Magnuson, T., Heard, E. and Chang, H. Y.** (2015). Systematic discovery of
641 Xist RNA binding proteins. *Cell* **161**, 404-416.
642 **Dimitrova, N., Zamudio, J. R., Jong, R. M., Soukup, D., Resnick, R., Sarma, K.,**
643 **Ward, A. J., Raj, A., Lee, J. T., Sharp, P. A., et al.** (2014). LincRNA-p21 activates
644 p21 in cis to promote polycomb target gene expression and to enforce the G1/S
645 checkpoint. *Mol Cell* **54**, 777-790.
646 **Figueroa, A., Cuadrado, A., Fan, J., Atasoy, U., Muscat, G. E., Muñoz-Canoves, P.,**

**Gorospe, M. and Muñoz, A.** (2003). Role of HuR in skeletal myogenesis through coordinate regulation of muscle differentiation genes. *Mol Cell Biol* **23**, 4991-5004.

**Gebauer, F., Schwarzl, T., Valcárcel, J. and Hentze, M. W.** (2021). RNA-binding proteins in human genetic disease. *Nat Rev Genet* **22**, 185-198.

**Gerstberger, S., Hafner, M. and Tuschl, T.** (2014). A census of human RNA-binding proteins. *Nat Rev Genet* **15**, 829-845.

**Harding, H. P., Zhang, Y., Zeng, H., Novoa, I., Lu, P. D., Calfon, M., Sadri, N., Yun, C., Popko, B., Paules, R., et al.** (2003). An integrated stress response regulates amino acid metabolism and resistance to oxidative stress. *Mol Cell* **11**, 619-633.

**Hetz, C., Chevet, E. and Oakes, S. A.** (2015). Proteostasis control by the unfolded protein response. *Nat Cell Biol* **17**, 829-838.

**Hirose, T., Yamazaki, T. and Nakagawa, S.** (2019). Molecular anatomy of the architectural NEAT1 noncoding RNA: The domains, interactors, and biogenesis pathway required to build phase - separated nuclear paraspeckles. *Wiley Interdiscip Rev Rna* **10**, e1545.

**Hitachi, K. and Tsuchida, K.** (2019). Data describing the effects of depletion of Myoparr, myogenin, Ddx17, and hnRNPK in differentiating C2C12 cells. *Data Brief* **25**, 104172.

**Hitachi, K. and Tsuchida, K.** (2020). The Chemical Biology of Long Noncoding RNAs. *Rna Technologies* 431-463.

**Hitachi, K., Nakatani, M., Takasaki, A., Ouchi, Y., Uezumi, A., Ageta, H., Inagaki, H., Kurahashi, H. and Tsuchida, K.** (2019). Myogenin promoter-associated lncRNA Myoparr is essential for myogenic differentiation. *Embo Rep* **20**, e47468.

**Hon, C.-C., Ramilowski, J. A., Harshbarger, J., Bertin, N., Rackham, O. J. L., Gough, J., Denisenko, E., Schmeier, S., Poulsen, T. M., Severin, J., et al.** (2017). An atlas of human long non-coding RNAs with accurate 5′ ends. *Nature* **543**, 199-204.

**Howarth, M. M., Simpson, D., Ngok, S. P., Nieves, B., Chen, R., Siprashvili, Z., Vaka, D., Breese, M. R., Crompton, B. D., Alexe, G., et al.** (2014). Long noncoding RNA EWSAT1-mediated gene repression facilitates Ewing sarcoma oncogenesis. *J Clin Invest* **124**, 5275-5290.

**Hulmi, J. J., Hentilä, J., DeRuisseau, K. C., Oliveira, B. M., Papaioannou, K. G., Autio, R., Kujala, U. M., Ritvos, O., Kainulainen, H., Korkmaz, A., et al.** (2016). Effects of muscular dystrophy, exercise and blocking activin receptor IIB ligands on

680 the unfolded protein response and oxidative stress. *Free Radical Bio Med* **99**, 308-
681 322.
682 **Ikezoe, K., Nakamori, M., Furuya, H., Arahata, H., Kanemoto, S., Kimura, T.,**
683 **Imaizumi, K., Takahashi, M. P., Sakoda, S., Fujii, N., et al.** (2007). Endoplasmic
684 reticulum stress in myotonic dystrophy type 1 muscle. *Acta Neuropathol* **114**, 527-
685 535.
686 **Jonas, K., Calin, G. A. and Pichler, M.** (2020). RNA-binding proteins as important
687 regulators of long non-coding RNAs in cancer. *Int J Mol Sci* **21**, 2969.
688 **Kanehisa, M., Furumichi, M., Sato, Y., Ishiguro-Watanabe, M. and Tanabe, M.**
689 (2020). KEGG: integrating viruses and cellular organisms. *Nucleic Acids Res* **49**,
690 D545-D551.
691 **Kataruka, S., Akhade, V. S., Kayyar, B. and Rao, M. R. S.** (2017). Mrhl long
692 noncoding RNA mediates meiotic commitment of mouse spermatogonial cells by
693 regulating Sox8 expression. *Mol Cell Biol* **37**, e00632-16.
694 **Kawaguchi, T., Tanigawa, A., Naganuma, T., Ohkawa, Y., Souquere, S., Pierron, G.**
695 **and Hirose, T.** (2015). SWI/SNF chromatin-remodeling complexes function in
696 noncoding RNA-dependent assembly of nuclear bodies. *Proc National Acad Sci* **112**,
697 4304-4309.
698 **Kelaini, S., Chan, C., Cornelius, V. A. and Margariti, A.** (2021). RNA-binding proteins
699 hold key roles in function, dysfunction, and disease. *Biology* **10**, 366.
700 **Legnini, I., Morlando, M., Mangiavacchi, A., Fatica, A. and Bozzoni, I.** (2014). A
701 feedforward regulatory loop between HuR and the long noncoding RNA linc-MD1
702 controls early phases of myogenesis. *Mol Cell* **53**, 506-514.
703 **Liu, R., Liu, H., Chen, X., Kirby, M., Brown, P. O. and Zhao, K.** (2001). Regulation
704 of CSF1 promoter by the SWI/SNF-like BAF complex. *Cell* **106**, 309-318.
705 **Love, M. I., Huber, W. and Anders, S.** (2014). Moderated estimation of fold change and
706 dispersion for RNA-seq data with DESeq2. *Genome Biol* **15**, 550.
707 **Lynch, M., Chen, L., Ravitz, M. J., Mehtani, S., Korenblat, K., Pazin, M. J. and**
708 **Schmidt, E. V.** (2005). hnRNP K binds a core polypyrimidine element in the
709 eukaryotic translation initiation Factor 4E (eIF4E) promoter, and its regulation of
710 eIF4E contributes to neoplastic transformation. *Mol Cell Biol* **25**, 6436-6453.
711 **Ma, L., Cao, J., Liu, L., Du, Q., Li, Z., Zou, D., Bajic, V. B. and Zhang, Z.** (2019).
712 LncBook: a curated knowledgebase of human long non-coding RNAs. *Nucleic Acids*

*Res* **47**, D128-D134.

**Makeyev, A. V. and Liebhaber, S. A.** (2002). The poly(C)-binding proteins: A multiplicity of functions and a search for mechanisms. *Rna* **8**, 265-278.

**Nakanishi, K., Sudo, T. and Morishima, N.** (2005). Endoplasmic reticulum stress signaling transmitted by ATF6 mediates apoptosis during muscle development. *J Cell Biology* **169**, 555-560.

**Nakanishi, K., Dohmae, N. and Morishima, N.** (2007). Endoplasmic reticulum stress increases myofiber formation in vitro. *Faseb J* **21**, 2994-3003.

**Nostrand, E. L. V., Freese, P., Pratt, G. A., Wang, X., Wei, X., Xiao, R., Blue, S. M., Chen, J.-Y., Cody, N. A. L., Dominguez, D., et al.** (2020). A large-scale binding and functional map of human RNA-binding proteins. *Nature* **583**, 711-719.

**Paz, I., Kosti, I., Ares, M., Cline, M. and Mandel-Gutfreund, Y.** (2014). RBPmap: a web server for mapping binding sites of RNA-binding proteins. *Nucleic Acids Res* **42**, W361-W367.

**Sallam, T., Jones, M., Thomas, B. J., Wu, X., Gilliland, T., Qian, K., Eskin, A., Casero, D., Zhang, Z., Sandhu, J., et al.** (2018). Transcriptional regulation of macrophage cholesterol efflux and atherogenesis by a long noncoding RNA. *Nat Med* **24**, 304-312.

**Schuster-Gossler, K., Cordes, R. and Gossler, A.** (2007). Premature myogenic differentiation and depletion of progenitor cells cause severe muscle hypotrophy in Delta1 mutants. *Proc National Acad Sci* **104**, 537-542.

**Shan, J., Zhang, F., Sharkey, J., Tang, T. A., Örd, T. and Kilberg, M. S.** (2016). The C/ebp-Atf response element (CARE) location reveals two distinct Atf4-dependent, elongation-mediated mechanisms for transcriptional induction of aminoacyl-tRNA synthetase genes in response to amino acid limitation. *Nucleic Acids Res* **44**, 9719-9732.

**Statello, L., Guo, C.-J., Chen, L.-L. and Huarte, M.** (2021). Gene regulation by long non-coding RNAs and its biological functions. *Nat Rev Mol Cell Bio* **22**, 96-118.

**Tang, S., Xie, Z., Wang, P., Li, J., Wang, S., Liu, W., Li, M., Wu, X., Su, H., Cen, S., et al.** (2018). LncRNA-OG promotes the osteogenic differentiation of bone marrow-derived mesenchymal stem cells under the regulation of hnRNPK. *Stem Cells* **37**, 270-283.

**Targoff, I. N., Trieu, E. P. and Miller, F. W.** (1993). Reaction of anti-OJ autoantibodies

with components of the multi-enzyme complex of aminoacyl-tRNA synthetases in addition to isoleucyl-tRNA synthetase. *J Clin Invest* **91**, 2556-2564.

**Wang, Z., Cui, J., Wong, W. M., Li, X., Xue, W., Lin, R., Wang, J., Wang, P., Tanner, J. A., Cheah, K. S. E., et al.** (2013). Kif5b controls the localization of myofibril components for their assembly and linkage to the myotendinous junctions. *Development* **140**, 617-626.

**Wang, Z., Qiu, H., He, J., Liu, L., Xue, W., Fox, A., Tickner, J. and Xu, J.** (2020). The emerging roles of hnRNPK. *J Cell Physiol* **235**, 1995-2008.

**Xiong, G., Hindi, S. M., Mann, A. K., Gallot, Y. S., Bohnert, K. R., Cavener, D. R., Whittemore, S. R. and Kumar, A.** (2017). The PERK arm of the unfolded protein response regulates satellite cell-mediated skeletal muscle regeneration. *Elife* **6**, e22871.

**Xu, Y., Li, R., Zhang, K., Wu, W., Wang, S., Zhang, P. and Xu, H.** (2018). The multifunctional RNA-binding protein hnRNPK is critical for the proliferation and differentiation of myoblasts. *BMB Rep* **51**, 350-355.

**Yano, M., Okano, H. J. and Okano, H.** (2005). Involvement of Hu and heterogeneous nuclear ribonucleoprotein K in neuronal differentiation through p21 mRNA post-transcriptional regulation. *J Biol Chem* **280**, 12690-12699.

**Yoon, J.-H., Abdelmohsen, K., Srikantan, S., Yang, X., Martindale, J. L., De, S., Huarte, M., Zhan, M., Becker, K. G. and Gorospe, M.** (2012). LincRNA-p21 suppresses target mRNA translation. *Mol Cell* **47**, 648-655.

**Zhou, Y., Zhou, B., Pache, L., Chang, M., Khodabakhshi, A. H., Tanaseichuk, O., Benner, C. and Chanda, S. K.** (2019). Metascape provides a biologist-oriented resource for the analysis of systems-level datasets. *Nat Commun* **10**, 1523.

Figure 1



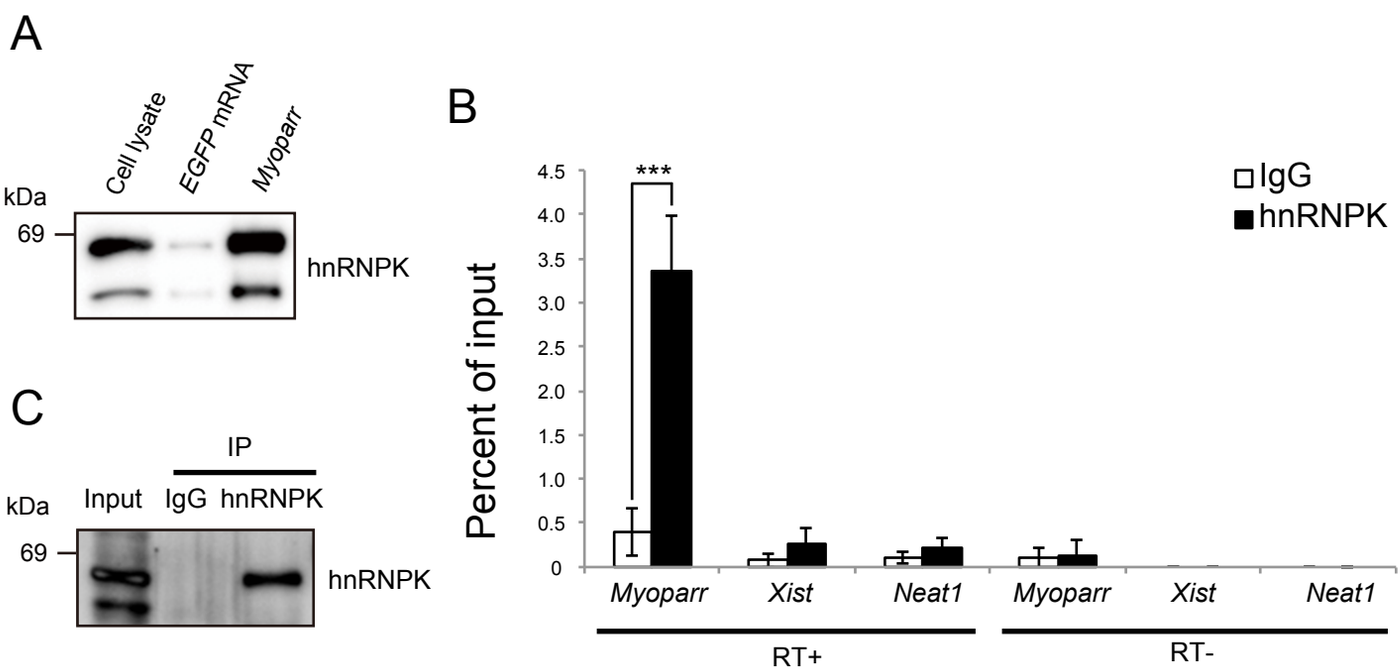

# Figure 2

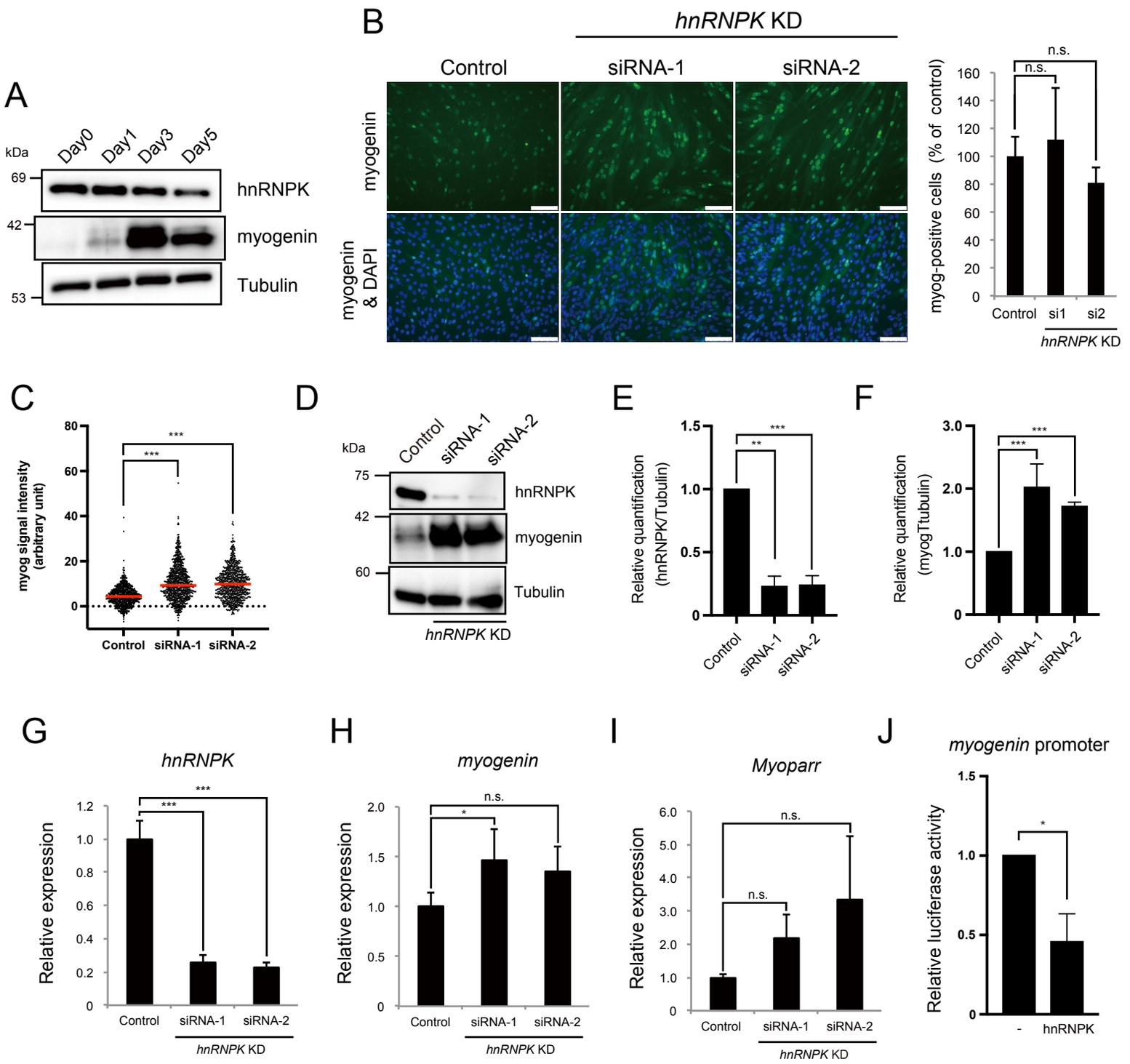

# Figure 3

A

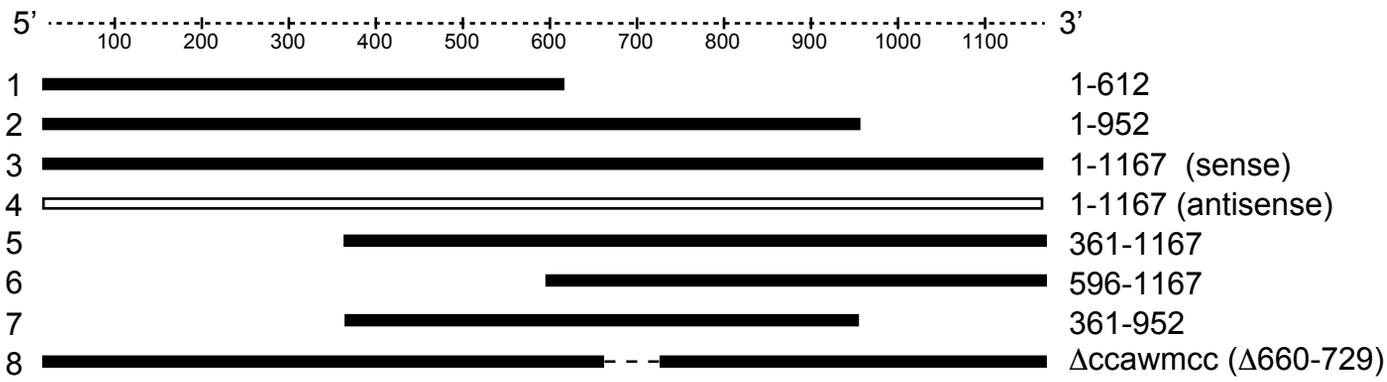


B

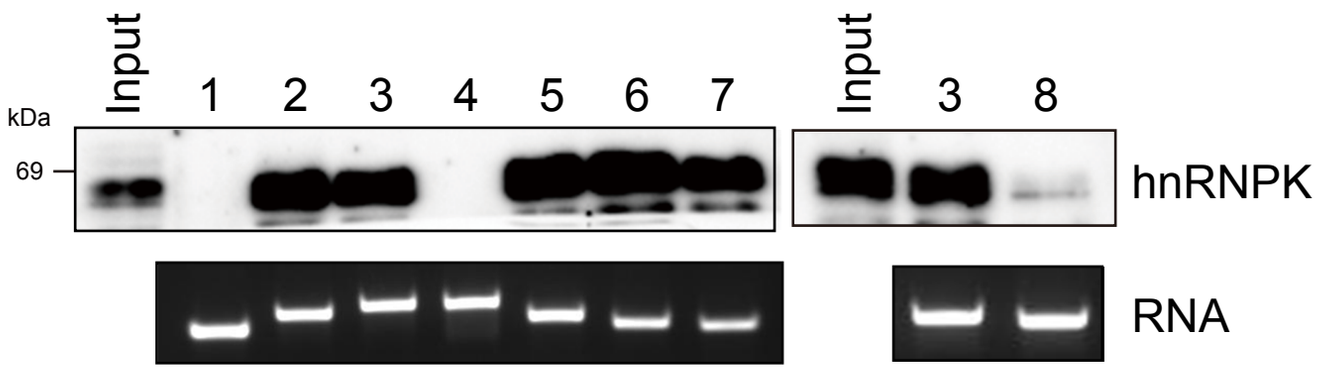


C

**Protein: HNRNPK(Hs/Mm)**

| Position | Motif | Occurrence | Z-score | P-value |
|---|---|---|---|---|
| 274 | ccawmcc | gucaguccc**augagacccc**uaaaga**ccuacca**cuaccacaucaggaccacuccagau | 2.420 | 7.76e-03 |
| 295 | ccawmcc | aagaccuaccacuaccacaucagga**ccacucc**agauuuggggcgugugugugugugu | 2.435 | 7.45e-03 |
| 674 | ccawmcc | auuuucuucauuuacauuucaaaug**cuauccc**aaaaguucccuauacccccccuccc | 2.884 | 1.96e-03 |
| 690 | ccawmcc | uuucaaaugcuauccc**aaaaguucc**c**uauacc**ccccccuccccccgcccugcucccu | 2.986 | 1.41e-03 |
| 695 | ccawmcc | aaugcuauccc**aaaaguucc**cuaua**ccccccc**uccccccgcccugcucccuaccca | 2.957 | 1.55e-03 |
| 699 | ccawmcc | cuauccc**aaaaguucc**cuauacccc**cccucccc**cccgcccugcucccuacccacuca | 3.246 | 5.85e-04 |
| 700 | ccawmcc | uauccc**aaaaguucc**cuauacccc**ccucccc**ccgcccugcucccuacccacucau | 3.000 | 1.35e-03 |
| 706 | ccawmcc | aaaaguucccuauacccccccuccc**cccgccc**ugcucccuacccacucauucccac | 3.000 | 1.35e-03 |
| 718 | ccawmcc | uacccccccucccccgcccugcuc**cccuacc**cacucauucccacuucuuggcccug | 2.957 | 1.55e-03 |
| 719 | ccawmcc | acccccccucccccgcccugcucc**ccuaccc**acucauucccacuucuuggcccugg | 3.319 | 4.52e-04 |

D

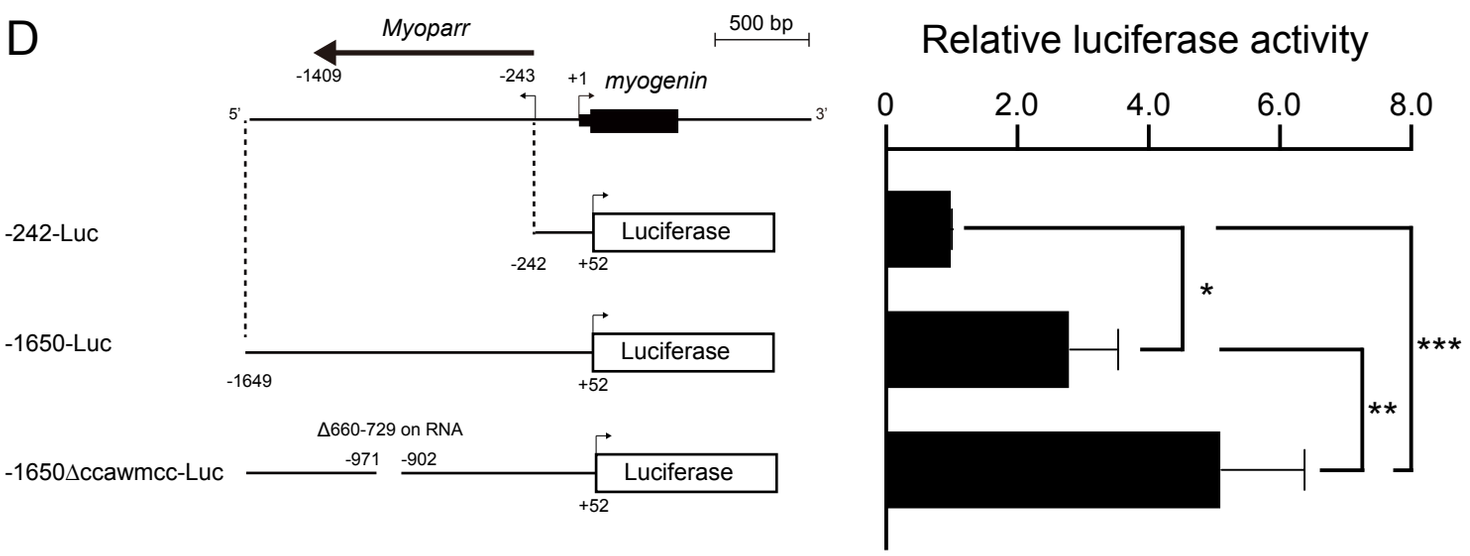

# Figure 4



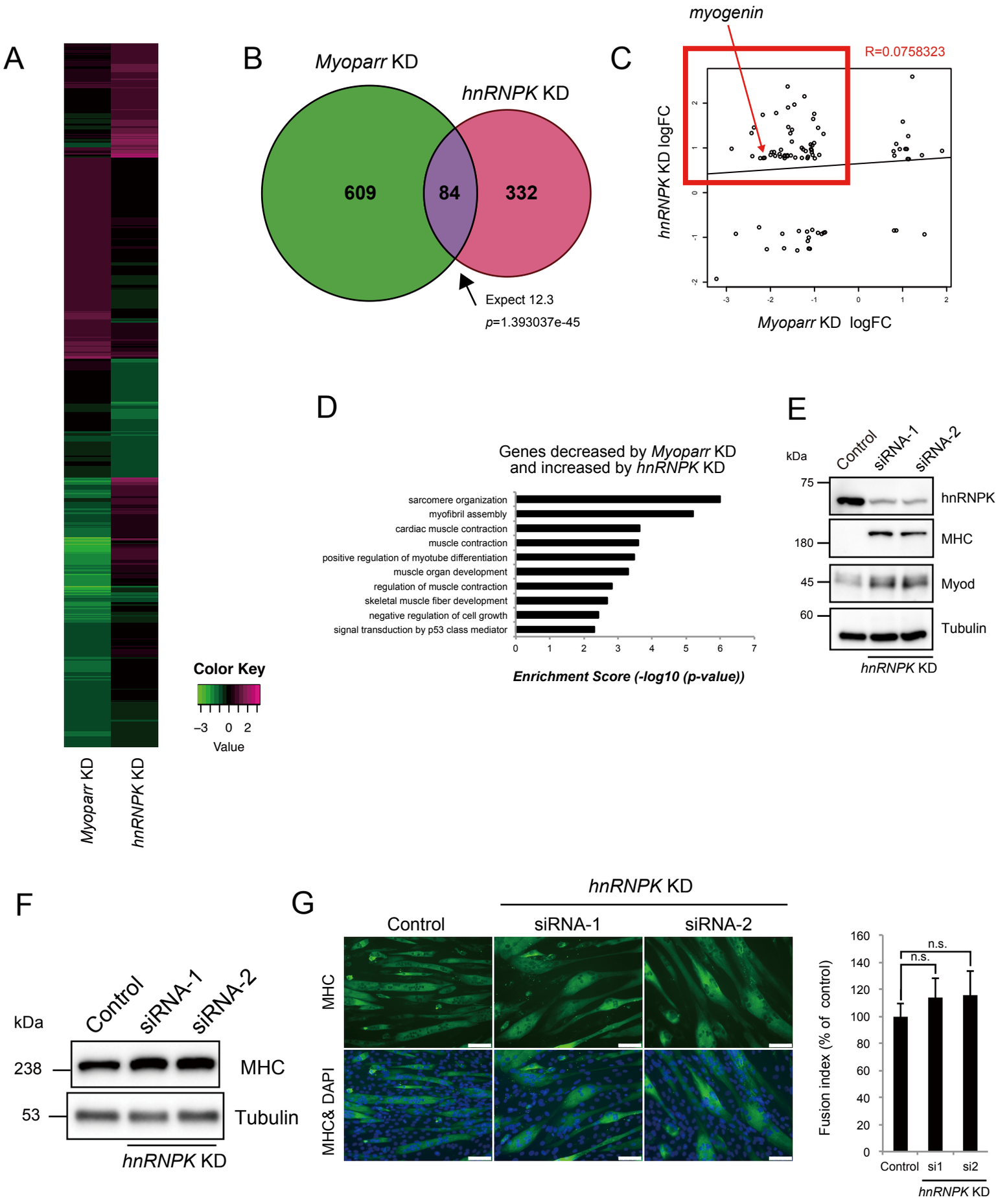

# Figure 5

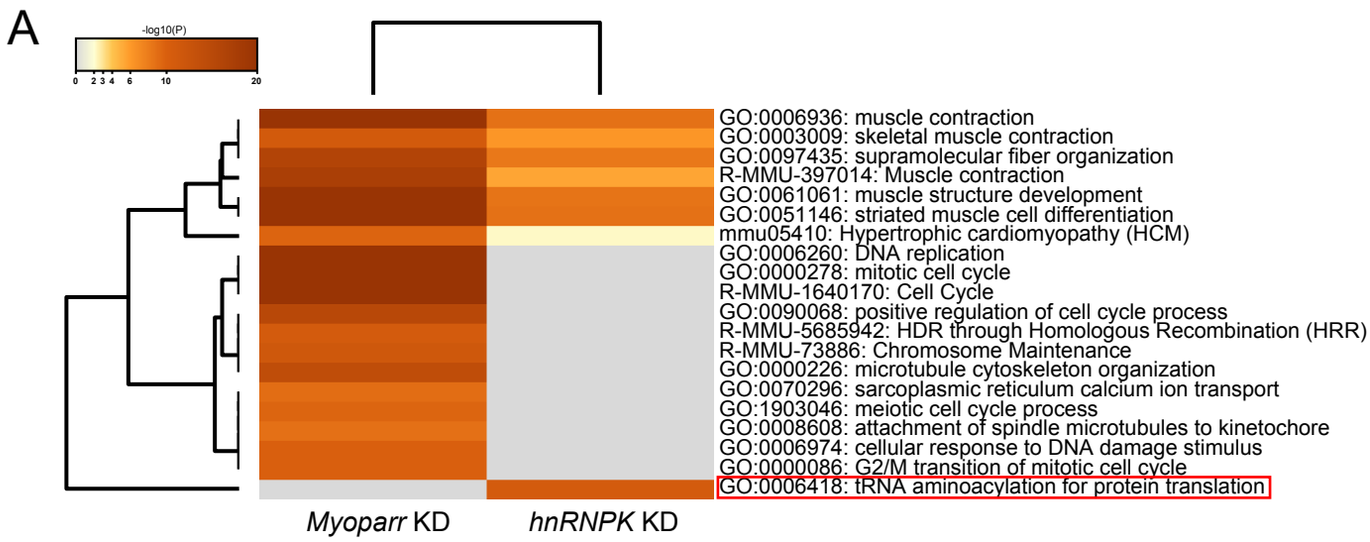


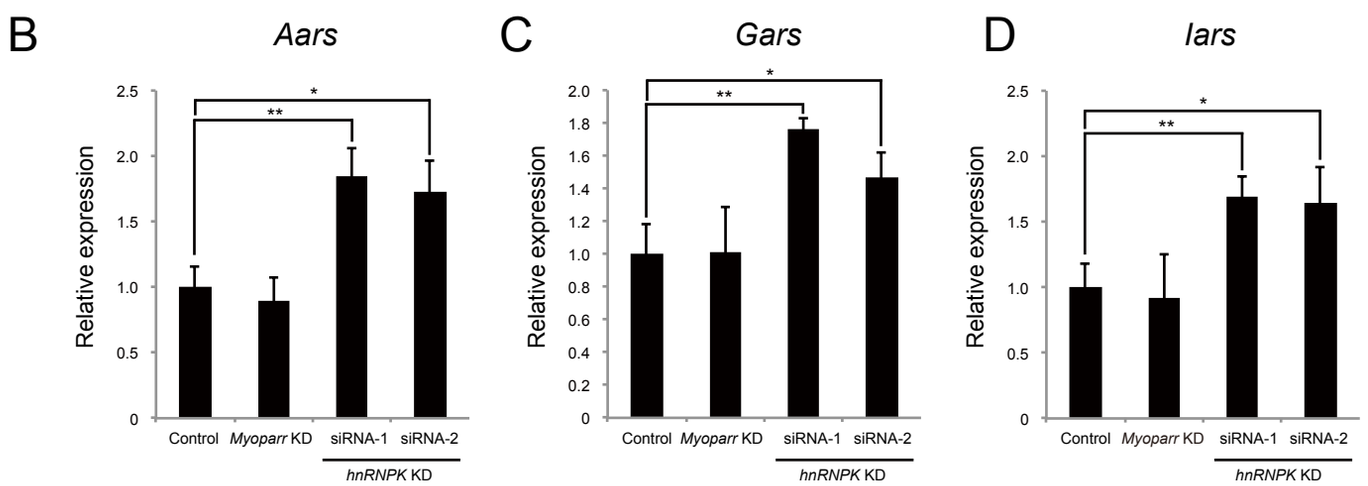


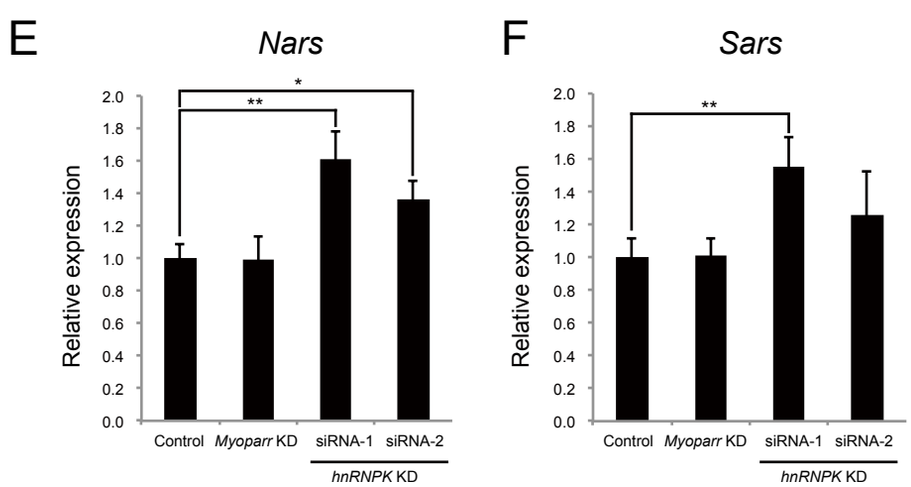


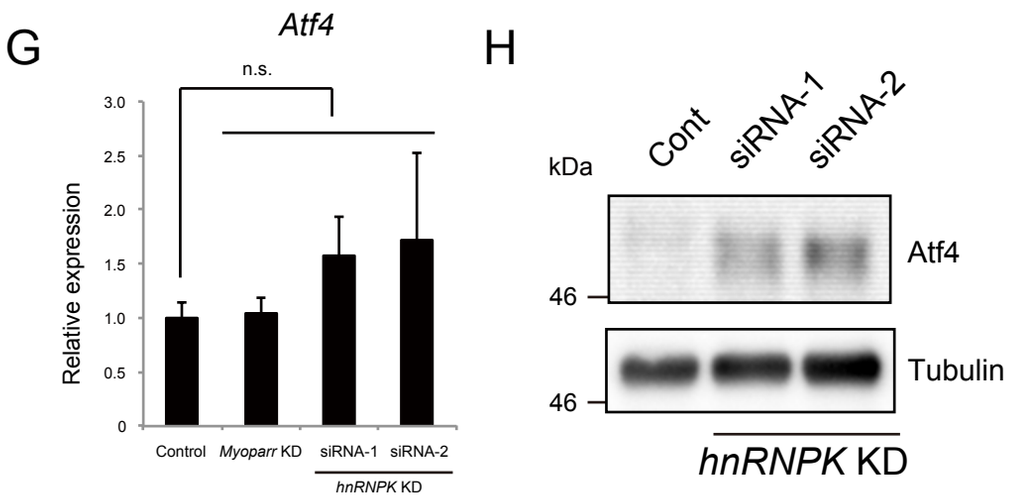

Figure 6



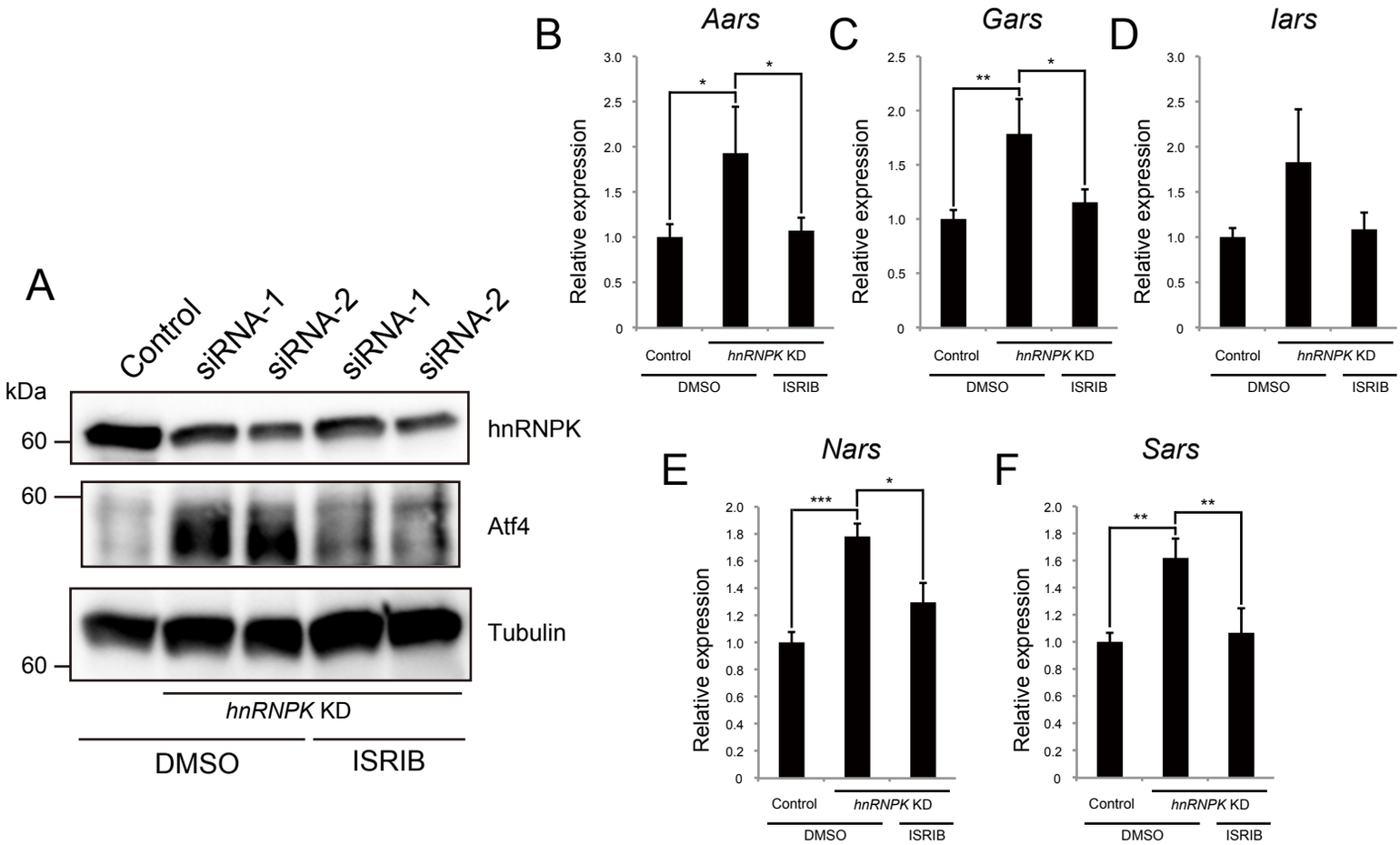

Figure 7